

Supernovae Ia Constraints on a Time-Variable Cosmological “Constant”

Silviu Podariu and Bharat Ratra

Department of Physics, Kansas State University, Manhattan, KS 66506.

ABSTRACT

The energy density of a scalar field ϕ with potential $V(\phi) \propto \phi^{-\alpha}$, $\alpha > 0$, behaves like a time-variable cosmological constant that could contribute significantly to the present energy density. Predictions of this spatially-flat model are compared to recent Type Ia supernovae apparent magnitude versus redshift data. A large region of model parameter space is consistent with current observations. (These constraints are based on the exact scalar field model equations of motion, not on the widely used time-independent equation of state fluid approximation equations of motion.) We examine the consequences of also incorporating constraints from recent measurements of the Hubble parameter and the age of the universe in the constant and time-variable cosmological constant models. We also study the effect of using a non-informative prior for the density parameter.

Subject headings: supernovae: general—cosmology: observations—large-scale structure of the universe

1. Introduction

Current observations are more consistent with low-density cold dark matter (CDM) dominated cosmogonies. For recent discussions see, e.g., Ratra et al. (1999a), Kravtsov & Klypin (1999), Doroshkevich et al. (1999), Colley et al. (2000), Freudling et al. (1999), Sahni & Starobinsky (1999), Bahcall et al. (1999), and Donahue & Voit (1999). The simplest low-density CDM models have either flat spatial hypersurfaces and a constant or time-variable cosmological “constant” Λ (see, e.g., Peebles 1984; Peebles & Ratra 1988, hereafter PR; Efstathiou, Sutherland, & Maddox 1990; Stompor, Górski, & Banday 1995; Caldwell, Dave, & Steinhardt 1998), or open spatial hypersurfaces and no Λ (see, e.g., Gott 1982, 1997; Ratra & Peebles 1994, 1995; Górski et al. 1998).

While these models are consistent with most recent observations, there are notable exceptions. For instance, recent applications of the apparent magnitude versus redshift test based on Type Ia supernovae favor a non-zero Λ (see, e.g., Riess et al. 1998, hereafter R98; Perlmutter et al. 1999a, hereafter P99), although not with great statistical significance (Drell, Loredo, & Wasserman 1999).

On the other hand, the open model is favored by:

- Measurements of the Hubble parameter H_0 ($= 100h$ km s $^{-1}$ Mpc $^{-1}$) which indicate $h = 0.65 \pm 0.1$ at 2σ (see, e.g., Suntzeff et al. 1999; Biggs et al. 1999; Madore et al. 1999), and measurements of the age of the universe which indicate $t_0 = 12 \pm 2.5$ Gyr at 2σ (see, e.g., Reid 1997; Gratton et al. 1997; Chaboyer et al. 1998). This is because the resulting central $H_0 t_0$ value is consistent with a low-density open model with nonrelativistic-matter density parameter $\Omega_0 \approx 0.35$ and requires a rather large $\Omega_0 \approx 0.6$ in the flat-constant- Λ case.
- Analyses of the rate of gravitational lensing of quasars and radio sources by foreground galaxies which require a large $\Omega_0 \geq 0.38$ at 2σ in the flat-constant- Λ model (see, e.g., Falco, Kochanek, & Muñoz 1998).
- Analyses of the number of large arcs formed by strong gravitational lensing by clusters (Bartelmann et al. 1998; Meneghetti et al. 1999).
- The need for mild anti-biasing to accommodate the excessive intermediate- and small-scale power predicted in the DMR normalized flat-constant- Λ CDM model with a scale-invariant spectrum (see, e.g., Cole et al. 1997).

While the time-variable Λ model has not yet been studied to the same extent as the open and flat- Λ cases, it is likely that it can be reconciled with most of these observations (see, e.g., PR; Ratra & Quillen 1992, hereafter RQ; Frieman & Waga 1998; Perlmutter, Turner, & White 1999b; Wang et al. 1999; Efstathiou 1999).

We emphasize that most of these observational indications are tentative and certainly not definitive. This is particularly true for constraints derived from a χ^2 comparison between model predictions and cosmic microwave background (CMB) anisotropy measurements (see, e.g., Ganga, Ratra, & Sugiyama 1996; Lineweaver & Barbosa 1998; Baker et al. 1999; Rocha 1999), see discussions in Bond, Jaffe, & Knox (1998) and Ratra et al. (1999b). More reliable constraints follow from models-based maximum likelihood analyses of the CMB anisotropy data (see, e.g., Górski et al. 1995; Yamamoto & Bunn 1996; Ganga et al. 1998; Ratra et al. 1999b; Rocha et al. 1999), which make use of all the information in the CMB anisotropy data and are based on fewer approximations. However, this technique has not yet been used to analyze enough data sets to provide robust statistical constraints. Kamionkowski & Kosowsky (1999) review what might be expected from the CMB anisotropy in the near future.

In this paper we examine constraints on a constant and time-variable Λ that follow from recent Type Ia supernovae apparent magnitude versus redshift data and recent measurements of H_0 and t_0 . We focus here on the favored scalar field (ϕ) model for a time-variable Λ (PR; Ratra & Peebles 1988, hereafter RP), in which the scalar field potential $V(\phi) \propto \phi^{-\alpha}$, $\alpha > 0$, at low redshift¹. This scalar

¹Other potentials have been considered, e.g., an exponential potential (see, e.g., Lucchin & Matarrese 1985; RP; Ratra 1992; Wetterich 1995; Ferreira & Joyce 1998), or one that gives rise to an ultra-light pseudo-Nambu-Goldstone boson (see, e.g., Frieman et al. 1995; Frieman & Waga 1998), but such models are either inconsistent with observations

field could have played the role of the inflaton at much higher redshift, with the potential $V(\phi)$ dropping to a non-zero value at the end of inflation and then decaying more slowly with increasing ϕ (PR; RP). See Peebles & Vilenkin (1999), Perrotta & Baccigalupi (1999) and Giovannini (1999) for a specific model and observational consequences of this scenario. A potential $\propto \phi^{-\alpha}$ could arise in a number of high energy particle physics models, see, e.g., Binétruy (1999), Kim (1999), Barr (1999), Choi (1999), Banks, Dine, & Nelson (1999), Brax & Martin (1999), Masiero, Pietroni, & Rosati (1999), and Bento & Bertolami (1999) for specific examples. It is conceivable that such a setting might provide an explanation for the needed form of the potential, as well as for the needed very weak coupling of ϕ to other fields (RP; Carroll 1998; Kolda & Lyth 1999, but see Perival 1999 and Garriga, Livio, & Vilenkin 1999 for other possible explanations for the needed present value of Λ).

A scalar field is mathematically equivalent to a fluid with a time-dependent speed of sound (Ratra 1991). This equivalence may be used to show that a scalar field with potential $V(\phi) \propto \phi^{-\alpha}$, $\alpha > 0$, acts like a fluid with negative pressure and that the ϕ energy density behaves like a cosmological constant that decreases with time. This energy density could come to dominate at low redshift and thus help reconcile low dynamical estimates of the mean mass density with a spatially-flat cosmological model. Alternate mechanisms that also rely on negative pressure to achieve this result have been discussed (see, e.g., Özer & Taha 1986; Freese et al. 1987; Turner & White 1997; Chiba, Sugiyama, & Nakamura 1997; Özer 1999; Waga & Miceli 1999; Overduin 1999; Bucher & Spergel 1999). However, these mechanisms are either inconsistent or do not share a very appealing feature of the scalar field models. For some of the scalar field potentials mentioned above, the solution of the equations of motion is an attractive time-dependent fixed point (RP; PR; Wetterich 1995; Ferreira & Joyce 1998; Copeland, Liddle, & Wands 1998; Zlatev, Wang, & Steinhardt 1999; Liddle & Scherrer 1999; Santiago & Silbergleit 1998; Uzan 1999). This means that for a wide range of initial conditions the scalar field ϕ evolves in a manner that ensures that the cosmological constant contributes a reasonable energy density at low redshift. Of course, this does not resolve the (quantum-mechanical) cosmological constant problem.

There have been many studies of the constraints placed on a time-variable Λ from Type Ia supernovae apparent magnitude versus redshift data (see, e.g., Turner & White 1997; Frieman & Waga 1998; Garnavich et al. 1998; Hu et al. 1999; Cooray 1999; Waga & Miceli 1999; P99; Perlmutter et al. 1999b; Wang et al. 1999; Efstathiou 1999). However, except for the analysis of Frieman & Waga (1998), who use the earlier Perlmutter et al. (1997) data, these analyses have mostly made use of the time-independent equation of state fluid approximation to the scalar field model for a time-variable Λ (Perlmutter et al. 1999b and Efstathiou 1999 do go beyond the time-independent equation of state approximation by also approximating the time dependence of the equation of state, however, they do not analyze the exact scalar field model)². A major purpose

or do not share the more promising features of the inverse power law potential model.

²A similar criticism holds for most analyses of the constraints on a time-variable Λ from gravitational lensing

of this paper is to use the newer supernovae data of R98 and P99 to derive constraints on a time-variable Λ without making use of the time-independent equation of state fluid approximation to the scalar field model.

In the analyses here we use the most recent R98 and P99 data to place constraints on a constant and time-variable Λ . We note, however, that this is a young field and insufficient understanding of a number of astrophysical processes and effects (the mechanism responsible for the supernova, evolution, environmental effects, intergalactic dust, etc.) could render this a premature undertaking (see, e.g., Höflich, Wheeler, & Thielemann 1998; Aguirre 1999; Drell et al. 1999; Umeda et al. 1999; Riess et al. 1999; Wang 1999). Furthermore, other cosmological explanations (time-variable gravitational or fine structure “constants”) could be consistent with the data (see, e.g., Amendola, Corasaniti, & Occhionero 1999; Barrow & Magueijo 1999; García-Berro et al. 1999).

In addition to analyzing just the supernovae data, we also incorporate constraints from recent measurements of H_0 and t_0 and derive a combined likelihood function which we use to constrain both a constant and a time-variable Λ . We also examine the effect on the model-parameter constraints caused by varying the prior for Ω_0 .

We emphasize that the tests examined in this paper are not sensitive to the spectrum of inhomogeneities in the models considered. This spectrum (possibly generated by quantum mechanical zero-point fluctuations during inflation, see, e.g., Fischler, Ratra, & Susskind 1985) is relevant for some of the other tests mentioned above (CMB anisotropy, anti-biasing, etc.).

In §2 we summarize the computations. Results are presented and discussed in §3. Conclusions are given in §4.

2. Computation

We examine three sets of supernovae apparent magnitudes. We use the MLCS magnitudes for the R98 data, both including and excluding the unclassified SN 1997ck at $z = 0.97$ (with 50 and 49 SNe Ia, respectively). The third set are the corrected/effective stretch factor magnitudes for the 54 Fit C SNe Ia of P99. In all three cases we assume that the measured magnitudes are independent. We also assume that SNe Ia at high and low z are not significantly different (Drell et al. 1999, Riess et al. 1999, and Wang 1999 consider the possibility and consequences of evolution), and that intergalactic dust has a negligible effect (Aguirre 1999 considers the effects of dust).

Our analysis of the R98 data is similar to that described in their §4, with a few minor modifications. For the time-independent Λ model we compute the likelihood function $L(\Omega_0, \Omega_\Lambda, H_0)$ for a range of Ω_0 spanning the interval 0 to 2.5 in steps of 0.1, for a range of Ω_Λ spanning the interval

statistics (see, e.g., Bloomfield Torres & Waga 1996; Jain et al. 1998; Cooray 1999; Waga & Miceli 1999; Wang et al. 1999), with the exception of the analysis of RQ.

–1 to 3 in steps of 0.1, and for a range of H_0 spanning the interval 50 to 80 km s⁻¹ Mpc⁻¹ in steps of 0.5 km s⁻¹ Mpc⁻¹.

Our analysis of the P99 data is similar to theirs, with some modifications. Specifically, we work with their corrected/effective magnitudes and so need only compute a three-dimensional likelihood function $L(\Omega_0, \Omega_\Lambda, \mathcal{M}_B)$. Here \mathcal{M}_B is their “Hubble-constant-free” B band absolute magnitude (see P99) related to H_0 by $\mathcal{M}_B = -19.46 - 5\log_{10}H_0 + 25$ (determined by us from results in P99). For the time-independent Λ model we compute this likelihood function for a range of Ω_0 spanning the interval 0 to 3 in steps of 0.1, for a range of Ω_Λ spanning the interval –1.5 to 3 in steps of 0.1, and for a range of \mathcal{M}_B spanning the interval –3.95 to –2.95 in steps of 0.05 (which corresponds to about the same interval in H_0 used in our analyses of the R98 data). Note that in our P99 time-independent Λ model plots we do not show the likelihood for the whole $\Omega_0 - \Omega_\Lambda$ region over which we have computed it.

The spatially-flat time-variable Λ model we consider is the scalar field model with potential $V(\phi) \propto \phi^{-\alpha}$, $\alpha > 0$. When $\alpha \rightarrow 0$ the model tends to the flat-constant- Λ case and when $\alpha \rightarrow \infty$ it approaches the Einstein-de Sitter model. It is discussed in detail in PR, RP, and RQ, and we derive the predicted distance moduli for the SNe using expressions given in these papers.

As shown in these papers, the scalar field behaves like a fluid with a constant (but different) equation of state in each epoch of the model. For instance, in the CDM and baryon dominated epoch of the model, it obeys the equation of state $p_\phi = w_\phi \rho_\phi$ (relating the pressure and energy density of the scalar field), where

$$w_\phi = -\frac{2}{\alpha + 2}, \tag{1}$$

see, e.g., RQ eq. (2) or see Zlatev et al. (1999) for a more recent derivation. We shall also have need for an average equation of state parameter, used by Perlmutter et al. (1999b) and Wang et al. (1999),

$$w_{\text{eff}} = \frac{\int_0^{a_0} da \Omega_\phi(a) w_\phi(a)}{\int_0^{a_0} da \Omega_\phi(a)} \tag{2}$$

where Ω_ϕ is the scalar field density parameter and a is the scale factor (with a_0 being the present value).

In this model, for the R98 data we compute the likelihood function $L(\Omega_0, \alpha, H_0)$, and for the P99 data the likelihood function $L(\Omega_0, \alpha, \mathcal{M}_B)$. In both cases we evaluate the likelihood function for a range of Ω_0 spanning the interval 0.05 to 0.95 in steps of 0.025, for a range of α spanning the interval 0 to 8 in steps of 0.5, and for the same range of H_0 or \mathcal{M}_B as in the time-independent Λ cases discussed above.

We marginalize these three-dimensional likelihood functions by integrating over H_0 (for the R98 data) or \mathcal{M}_B (for the P99 data) and derive two-dimensional likelihood functions, $L(\Omega_0, \Omega_\Lambda)$ for the constant Λ model and $L(\Omega_0, \alpha)$ for the spatially-flat time-variable Λ case. These two-dimensional likelihood functions are used to derive highest posterior density limits (see Ganga et

al. 1997 and references therein) in the $(\Omega_0, \Omega_\Lambda)$ or (Ω_0, α) planes. In what follows we consider 1, 2, and 3 σ confidence limits which include 68.27, 95.45, and 99.73% of the area under the likelihood function.

When marginalizing over a parameter or deriving a limit from the likelihood functions, we consider a number of different priors. We first consider a uniform prior in the parameter integrated over, set to zero outside the range considered for the parameter.

We also incorporate constraints from measurements which indicate $H_0 = 65 \pm 7 \text{ km s}^{-1} \text{ Mpc}^{-1}$ at 1 σ (see, e.g., Biggs et al. 1999; Madore et al. 1999), by using the prior

$$p(H_0) = \frac{1}{\sqrt{2\pi}\{7 \text{ km s}^{-1} \text{ Mpc}^{-1}\}} \exp\left[-\frac{\{H_0 - 65 \text{ km s}^{-1} \text{ Mpc}^{-1}\}^2}{2\{7 \text{ km s}^{-1} \text{ Mpc}^{-1}\}^2}\right], \quad (3)$$

and from measurements which indicate $t_0 = 12 \pm 1.3 \text{ Gyr}$ at 1 σ (i.e., 0.5 Gyr added to the globular cluster age estimate of Chaboyer et al. 1998)³, by using the prior

$$p(t_0) = \frac{1}{\sqrt{2\pi}\{1.3 \text{ Gyr}\}} \exp\left[-\frac{\{t_0(H_0, \Omega_0, \Omega_\Lambda) - 12 \text{ Gyr}\}^2}{2\{1.3 \text{ Gyr}\}^2}\right], \quad (4)$$

with α replacing Ω_Λ in this expression in the spatially-flat time-variable Λ case. Note that Figure 2 of Chaboyer et al. (1998) may be used to establish that a Gaussian prior of the form of eq. (4) is a good approximation to the shifted Monte Carlo globular cluster age distribution. See Ganga et al. (1997) for a discussion of Gaussian priors in a related context. This method of incorporating constraints from measurements of H_0 and t_0 is not identical to the classical $H_0 t_0$ cosmological test (see, e.g., §13 of Peebles 1993).

Finally, since Ω_0 is a positive quantity, we also consider the non-informative prior (Berger 1985)⁴,

$$p(\Omega_0) = \frac{1}{\Omega_0}. \quad (5)$$

Since Ω_0 is bounded from below by the observed lower limit on the baryon density parameter ($\sim 0.01 - 0.05$, depending on data used, see, e.g., Olive, Steigman, & Walker 1999), this prior does not result in an infinity.

³A more complete analysis would need to account for the uncertainty in this (0.5 Gyr) numerical value. This would likely weaken the effect of this prior.

⁴We thank R. Gott for emphasizing this prior; a more complete discussion of it may be found in Gott et al. (in preparation). I. Wasserman has noted that such a prior is probably more appropriate for a parameter that sets the scale for the problem, such as H_0 here (see §B.2 of Drell et al. 1999; §VII of Jaynes 1968 gives a more general discussion). It is however still of interest to determine how the conclusions depend on the choice of prior.

3. Results and Discussion

Figure 1 shows the posterior probability density distribution function (PDF) confidence contours for the time-variable Λ scalar field model, derived using the three data sets discussed above. Figure 1*d* shows that constraints from the three different data sets are quite consistent. At 2σ a large region of the parameter space of these spatially-flat models (with a constant or time-variable Λ) is consistent with the SNe Ia data. This data favors a smaller Ω_0 as α is increased from zero.

A fluid with a time-independent equation of state $p = w\rho$, $w < 0$, has often been used to approximate the scalar field with potential $V(\phi) \propto \phi^{-\alpha}$ in the time-variable Λ model. The solid lines in Figure 2*a* show the confidence contours for such a fluid model, derived using the P99 Fit C data. These confidence contours are consistent with those shown in Figure 1 of Perlmutter et al. (1999b) (but see discussion below), Figure 10 of Wang et al. (1999), and Figure 4 of Efstathiou (1999). The dashed lines in Figure 2*a* show the exact scalar field model contours of Figure 1*c*, transformed using the relation between w_ϕ and α in the CDM and baryon dominated epoch (eq. [1]), which comes to an end just before the present. The two sets of contours agree near $w \sim -1$, as they must since at $w = -1$ this is the flat- Λ model and Λ does behave exactly like a fluid with a time-independent equation of state. However, the two sets of confidence contours differ significantly at larger w . Since the scalar field w_ϕ eventually switches over to -1 (in the scalar field dominated epoch, RP), it is unclear what significance should be ascribed to this difference. We stress, however, that since the time-independent equation of state fluid model is an approximation to the time-variable Λ scalar field model, constraints on model-parameter values that are based on the fluid model approximation are only approximate (and possibly indicative). In passing, we note that Perlmutter et al. (1999b) use w_{eff} (eq. [2]) and not w to parametrize the fluid model constraints. Figure 2*b* shows contours of constant w_{eff} as a function of α and Ω_0 in the time-variable Λ scalar field model. In a large part of model parameter space w_{eff} is a sensitive function of both α and Ω_0 and hence is not the best parameter to use to describe the time-variable Λ scalar field model.

Figure 3 shows the effects of incorporating constraints based on H_0 and t_0 measurements (eqs. [3, 4]). Panel *a*) shows that adding the H_0 constraint does not significantly alter the contours derived from the SNe Ia data alone. This is expected since the value of H_0 used here is very close to the value that is indicated by the SNe Ia data (see R98). However, incorporating the t_0 constraint, $t_0 = 12 \pm 1.3$ Gyr at 1σ , does significantly shift the contours, panel *b*). This is because the SNe Ia data alone favor a higher t_0 , 14.2 ± 1.7 Gyr (R98), or 14.5 ± 1.0 (0.63/ h) Gyr (P99).

Figure 4 shows constraints on the time-variable Λ model, from the three different SNe Ia data sets used in conjunction with the H_0 and t_0 measurements (eqs. [3, 4]). The main effect of incorporating the H_0 and t_0 constraints is to increase the favored values of Ω_0 ; a weaker effect is the disfavoring of larger values of α . Even this extended set of data does not tightly constrain model-parameter values.

Figure 5 shows the corresponding constraints on the constant Λ model (from the SNe Ia, H_0 ,

and t_0 measurements). Again, the major effect of including the H_0 and t_0 data is to increase the favored values of Ω_0 . A weaker effect is that it reduces the odds against reasonable open models (Górski et al. 1998), but not by a large factor.

Figures 6 and 7 show the effects of using the non-informative prior, $1/\Omega_0$, of eq. (5). The major effect is a decrease in the favored values of Ω_0 . In the time-variable Λ case there is also a slight increase in the favored values of α (see Figure 6) while in the constant Λ case there is a mild reduction in the odds against reasonable open models (see Figure 7). If the PDF was narrower (i.e., if the error bars on the data were smaller), changing from the flat to the non-informative prior would not result in as large a change in the confidence contours.

4. Conclusion

Recent SNe Ia data do favor models with a constant or time-variable Λ over an open model without a Λ . However, this is not at a very high level of statistical significance. Also, the incomplete understanding of a number of astrophysical effects and processes (evolution, intergalactic dust, etc.) means that these results are preliminary and not yet definitive.

The constraints on the time-variable Λ model derived here are based on the exact scalar field model equations of motion, not on the widely used time-independent equation of state fluid approximation equations of motion.

We acknowledge the advice and assistance of R. Gott, B. Kirshner, L. Krauss, V. Periwai, S. Perlmutter, A. Riess, E. Sidky, M. Vogeley, and I. Wasserman, and are specially indebted to J. Peebles and T. Souradeep. We acknowledge helpful discussions with I. Waga who has also computed the PDF confidence contours for the time-variable Λ scalar field model, with results consistent with those found in this paper. We thank the referee, I. Wasserman, for a prompt and detailed report which helped us improve the manuscript. We acknowledge support from NSF CAREER grant AST-9875031.

REFERENCES

- Aguirre, A.N. 1999, *ApJ*, 512, L19
- Amendola, L., Corasaniti, S., & Occhionero, F. 1999, *astro-ph/9907222*
- Bahcall, N.A., Ostriker, J.P., Perlmutter, S., & Steinhardt, P.J. 1999, *Science*, 284, 1481
- Baker, J.C., et al. 1999, *MNRAS*, submitted
- Banks, T., Dine, M., & Nelson, A.E. 1999, *J. High Ener. Phys.*, 9906, 014
- Barr, S.M. 1999, *Phys. Lett. B*, 454, 92
- Barrow, J.D., & Magueijo, J. 1999, *astro-ph/9907354*
- Bartelmann, M., Huss, A., Colberg, J.M., Jenkins, A., & Pearce, F.R. 1998, *A&A*, 330, 1
- Bento, M.C., & Bertolami, O. 1999, *gr-qc/9905075*
- Berger, J.O. 1985, *Statistical Decision Theory and Bayesian Analysis* (New York: Springer-Verlag), 82
- Biggs, A.D., Browne, I.W.A., Helbig, P., Koopmans, L.V.E., Wilkinson, P.N., & Perley, R.A. 1999, *MNRAS*, 304, 349
- Binétruy, P. 1999, *Phys. Rev. D*, 60, 063502
- Bloomfield Torres, L.F., & Waga, I. 1996, *MNRAS*, 279, 712
- Bond, J.R., Jaffe, A.H., & Knox, L. 1998, *Phys. Rev. D*, 57, 2117
- Brax, P., & Martin, J. 1999, *Phys. Lett. B*, in press
- Bucher, M., & Spergel, D. 1999, *Phys. Rev. D*, 60, 043505
- Caldwell, R.R., Dave, R., & Steinhardt, P.J. 1998, *Phys. Rev. Lett.*, 80, 1582
- Carroll, S.M. 1998, *Phys. Rev. Lett.*, 81, 3067
- Chaboyer, B., Demarque, P., Kernan, P.J., & Krauss, L.M. 1998, *ApJ*, 494, 96
- Chiba, T., Sugiyama, N., & Nakamura, T. 1997, *MNRAS*, 289, L5
- Choi, K. 1999, *hep-ph/9902292*
- Cole, S., Weinberg, D.H., Frenk, C.S., & Ratra, B. 1997, *MNRAS*, 289, 37
- Colley, W.N., Gott, J.R., Weinberg, D.H., Park, C., & Berlind, A.A. 2000, *ApJ*, 529, in press
- Copeland, E.J., Liddle, A.R., & Wands, D. 1998, *Phys. Rev. D*, 57, 4686
- Cooray, A.R. 1999, *A&A*, 341, 653
- Donahue, M. & Voit, G.M. 1999, *ApJ*, 523, L137
- Doroshkevich, A.G., Müller, V., Retzlaff, J., & Turchaninov, V. 1999, *MNRAS*, 306, 575
- Drell, P.S., Loredó, T.J., & Wasserman, I. 1999, *ApJ*, in press
- Efstathiou, G. 1999, *MNRAS*, submitted

- Efstathiou, G., Sutherland, W.J., & Maddox, S.J. 1990, *Nature*, 348, 705
- Falco, E.E., Kochanek, C.S., & Muñoz, J.A. 1998, *ApJ*, 494, 47
- Ferreira, P.G., & Joyce, M. 1998, *Phys. Rev. D*, 58, 023503
- Fischler, W., Ratra, B., & Susskind, L. 1985, *Nucl. Phys. B*, 259, 730
- Freese, K., Adams, F.C., Frieman, J.A., & Mottola, E. 1987, *Nucl. Phys. B*, 287, 797
- Freudling, W., et al. 1999, *ApJ*, 523, 1
- Frieman, J.A., Hill, C.T., Stebbins, A., & Waga, I. 1995, *Phys. Rev. Lett.*, 75, 2077
- Frieman, J.A., & Waga, I. 1998, *Phys. Rev. D*, 57, 4642
- Ganga, K., Ratra, B., Gundersen, J.O., & Sugiyama, N. 1997, *ApJ*, 484, 7
- Ganga, K., Ratra, B., Lim, M.A., Sugiyama, N., & Tanaka, S.T. 1998, *ApJS*, 114, 165
- Ganga, K., Ratra, B., & Sugiyama, N. 1996, *ApJ*, 461, L61
- García-Berro, E., Gaztañaga, E., Isern, J., Benvenuto, O., & Althaus, L. 1999, *astro-ph/9907440*
- Garnavich, P.M., et al. 1998, *ApJ*, 509, 74
- Garriga, J., Livio, M., & Vilenkin, A. 1999, *astro-ph/9906210*
- Giovannini, M. 1999, *astro-ph/9903004*
- Górski, K.M., Ratra, B., Stompor, R., Sugiyama, N., & Banday, A.J. 1998, *ApJS*, 114, 1
- Górski, K.M., Ratra, B., Sugiyama, N., & Banday, A.J. 1995, *ApJ*, 444, L65
- Gott, J.R. 1982, *Nature*, 295, 304
- Gott, J.R. 1997, in *Critical Dialogues in Cosmology*, ed. N. Turok (Singapore: World Scientific), 519
- Gratton, R.G., Fusi Pecci, F., Carretta, E., Clementini, G., Corsi, C.E., & Lattanzi, M. 1997, *ApJ*, 491, 749
- Hu, W., Eisenstein, D.J., Tegmark, M., & White, M. 1999, *Phys. Rev. D*, 59, 023512
- Höflich, P., Wheeler, J.C., & Thielemann, F.K. 1998, *ApJ*, 495, 617
- Jain, D., Panchapakesan, N., Mahajan, S., & Bhatia, V.B. 1998, *ApJ*, submitted
- Jaynes, E.T. 1968, *IEEE Trans. Sys. Sci. Cyb.*, SSC-4, 227
- Kamionkowski, M. & Kosowsky, A. 1999, *Ann. Rev. Nucl. Part. Sci.*, in press
- Kim, J.E. 1999, *J. High. Ener. Phys*, 9905, 022
- Kolda, C. & Lyth, D.H. 1999, *Phys. Lett. B*, 458, 197
- Kravtsov, A.V., & Klypin, A.A. 1999, *ApJ*, 520, 437
- Liddle, A.R., & Scherrer, R.J. 1999, *Phys. Rev. D*, 59, 023509
- Lineweaver, C.H., & Barbosa, D. 1998, *ApJ*, 496, 624

- Lucchin, F., & Matarrese, S. 1985, *Phys. Rev. D*, 32, 1316
- Madore, B.F., et al. 1999, *ApJ*, 515, 29
- Masiero, A., Pietroni, M., & Rosati F. 1999, *Phys. Rev. D*, submitted
- Meneghetti, M., Bolzonella, M., Bartelmann, M., Moscardini, L., & Tormen, G. 1999, *MNRAS*, submitted
- Olive, K.A., Steigman, G., & Walker, T.P. 1999, *Phys. Rep.*, in press
- Overduin, J.M. 1999, *ApJ*, 517, L1
- Özer, M. 1999, *ApJ*, 520, 45
- Özer, M., & Taha, M.O. 1986, *Phys. Lett. B*, 171, 363
- Peebles, P.J.E. 1984, *ApJ*, 284, 439
- Peebles, P.J.E. 1993, *Principles of Physical Cosmology* (Princeton: Princeton University Press)
- Peebles, P.J.E., & Ratra, B. 1988, *ApJ*, 325, L17 (PR)
- Peebles, P.J.E., & Vilenkin, A. 1999, *Phys. Rev. D*, 59, 063505
- Periwal, V. 1999, *astro-ph/9906253*
- Perlmutter, S., et al. 1997, *ApJ*, 483, 565
- Perlmutter, S., et al. 1999a, *ApJ*, 517, 565 (P99)
- Perlmutter, S., Turner, M.S., & White, M. 1999b, *Phys. Rev. Lett.*, 83, 670
- Perrotta, F., & Baccigalupi, C. 1999, *Phys. Rev. D*, 59, 123508
- Ratra, B. 1991, *Phys. Rev. D*, 43, 3802
- Ratra, B. 1992, *Phys. Rev. D*, 45, 1913
- Ratra, B., Ganga, K., Stompor, R., Sugiyama, N., de Bernardis, P., & Górski, K.M. 1999a, *ApJ*, 510, 11
- Ratra, B., & Peebles, P.J.E. 1988, *Phys. Rev. D*, 37, 3406 (RP)
- Ratra, B., & Peebles, P.J.E. 1994, *ApJ*, 432, L5
- Ratra, B., & Peebles, P.J.E. 1995, *Phys. Rev. D*, 52, 1837
- Ratra, B., & Quillen, A. 1992, *MNRAS*, 259, 738 (RQ)
- Ratra, B., Stompor, R., Ganga, K., Rocha, G., Sugiyama, N., & Górski, K.M. 1999b, *ApJ*, 517, 549
- Reid, I.N. 1997, *AJ*, 114, 161
- Riess, A.G., et al. 1998, *AJ*, 116, 1009 (R98)
- Riess, A.G., Filippenko, A.V., Li, W., & Schmidt, B.P. 1999, *AJ*, in press
- Rocha, G. 1999, in *Dark Matter in Astrophysics and Particle Physics 1998*, ed. H.V. Klapdor-Kleingrothaus & L. Baudis (Bristol: Institute of Physics Publishing), 238

- Rocha, G., Stompor, R., Ganga, K., Ratra, B., Platt, S.R., Sugiyama, N., & Górski, K.M. 1999, ApJ, 525, in press, astro-ph/9905127
- Sahni, V., & Starobinsky, A. 1999, Int. J. Mod. Phys. D, in press
- Santiago, D.I., & Silbergleit, A.S. 1998, Phys. Lett. A, submitted
- Stompor, R., Górski, K.M., & Banday, A.J. 1995, MNRAS, 277, 1225
- Suntzeff, N.B., et al. 1999, AJ, 117, 1175
- Turner, M.S., & White, M. 1997, Phys. Rev. D, 56, 4439
- Umeda, H., Nomoto, K., Kobayashi, C., Hachisu, I., & Kato, M. 1999, ApJ, 522, L43
- Uzan, J.-P. 1999, Phys. Rev. D, 59, 123510
- Waga, I., & Miceli, A.P.M.R. 1999, Phys. Rev. D, 59, 103507
- Wang, L., Caldwell, R.R., Ostriker, J.P., & Steinhardt, P.J. 1999, ApJ, submitted
- Wang, Y. 1999, ApJ, submitted
- Wetterich, C. 1995, A&A, 301, 321
- Yamamoto, K., & Bunn, E.F. 1996, ApJ, 464, 8
- Zlatev, I., Wang, L., & Steinhardt, P.J. 1999, Phys. Rev. Lett., 82, 896

Figure Captions

Fig. 1.– PDF confidence contours for the spatially-flat time-variable Λ scalar field model, with potential $V(\phi) \propto \phi^{-\alpha}$, derived using the three SNe Ia data sets. The $\alpha = 0$ axis corresponds to the spatially-flat time-independent Λ case. Confidence contours in panels *a) – c)* run from -2 to $+3 \sigma$ starting from the lower left hand corner of each panel. Panel *a)* shows those derived from all the R98 SNe, while *b)* is for R98 SNe excluding the $z = 0.97$ one, and *c)* is for the P99 Fit C data set. Panel *d)* compares the $\pm 2 \sigma$ limits from the three data sets: all R98 SNe (long-dashed lines); R98 SNe excluding the $z = 0.97$ one (short-dashed lines); and the P99 Fit C SNe (dotted lines).

Fig. 2.– *a)* PDF confidence contours derived from the P99 Fit C SNe, for a spatially-flat fluid model with equation of state $p = w\rho$ (solid lines show contours from -3 to $+3 \sigma$ starting from the lower left hand corner) and for the spatially-flat time-variable Λ scalar field model with potential $V(\phi) \propto \phi^{-\alpha}$ which behaves like a fluid model with equation of state $p_\phi = w_\phi \rho_\phi$ in the CDM and baryon dominated epoch (dotted lines show contours from -2 to $+3 \sigma$ starting from the lower left hand corner). The scalar field model contours were derived by using eq. (1) to transform the vertical axis of Figure 1*c)*. The fluid model likelihood function was computed for the full range of w and Ω_0 shown. The dot-dashed lines bound the $w_\phi - \Omega_0$ region that corresponds to the $\alpha - \Omega_0$ region of Figure 1*c)* over which the scalar field model likelihood was computed. *b)* Contours of constant w_{eff} (eq. [2]) in the $\alpha - \Omega_0$ plane for the time-variable Λ scalar field model with potential $V(\phi) \propto \phi^{-\alpha}$. Starting at the lower left hand corner, the contours correspond to $w_{\text{eff}} = -0.9, -0.8, -0.7, -0.6, -0.5, -0.4, -0.35, -0.3,$ and -0.25 .

Fig. 3.– PDF confidence contours derived from the P99 Fit C SNe, for the spatially-flat time-variable Λ scalar field model with potential $V(\phi) \propto \phi^{-\alpha}$. The dotted lines in panels *a) – c)* show the -2 to $+3 \sigma$ contours of Figure 1*c)*. The solid lines in these panels show the corresponding contours derived from the SNe data in conjunction with: *a)* H_0 measurements (using eq. [3]); *b)* t_0 measurements (using eq. [4]); and *c)* H_0 and t_0 measurements (using eqs. [3, 4]). Panel *d)* compares the $\pm 2 \sigma$ confidence contours from the SNe data in conjunction with: the H_0 constraint (long-dashed lines); the t_0 constraint (short-dashed lines); and both constraints (dotted lines).

Fig. 4.– PDF confidence contours for the spatially-flat time-variable Λ scalar field model, with potential $V(\phi) \propto \phi^{-\alpha}$, derived using the three SNe Ia data sets. Panel *a)* shows those derived from all the R98 SNe, while *b)* is from the R98 SNe excluding the $z = 0.97$ one, and *c)* is for the P99 Fit C data. Solid (dotted) lines in *a) – c)* are the 1, 2, and 3 σ contours from the SNe data with (without) the H_0 and t_0 constraints (eqs. [3, 4]); the dotted lines here are the solid lines in Figure 1*a) – c)*. Panel *d)* compares the $\pm 2 \sigma$ limits from the H_0 and t_0 constraints used in conjunction with: all R98 SNe (long-dashed lines); R98 SNe excluding the $z = 0.97$ one (short-dashed lines); and the P99 Fit C SNe (dotted lines).

Fig. 5.– PDF confidence contours for the time-independent Λ model, derived using the three SNe Ia data sets. Panel *a)* shows those derived from all the R98 SNe, while *b)* is from the R98 SNe

excluding the $z = 0.97$ one, and c) is for the P99 Fit C SNe. Solid (dotted) lines in $a) - c$) are the 1, 2, and 3 σ contours from the SNe data with (without) the H_0 and t_0 constraints (eqs. [3, 4]). Panel d) compares the $\pm 2 \sigma$ limits from the H_0 and t_0 constraints used in conjunction with: all R98 SNe (long-dashed lines); R98 SNe excluding the $z = 0.97$ one (short-dashed lines); and the P99 Fit C SNe (dotted lines). In all panels, models with parameter values in the upper left hand corner region bounded by the diagonal dot-dashed curve do not have a big bang. The horizontal dot-dashed line demarcates models with a zero Λ and the diagonal dot-dashed line running from $\Omega_\Lambda = 1$ to $\Omega_0 = 2$ corresponds to spatially-flat models.

Fig. 6.– PDF confidence contours (1, 2, and 3 σ) derived from the P99 Fit C SNe, for the spatially-flat time-variable Λ scalar field model. Panel $a)(b)$) ignores (accounts for) the H_0 and t_0 constraints (eqs. [3, 4]). The solid (dotted) lines use the non-informative $1/\Omega_0$ (flat) prior. The dotted lines in $a)(b)$) are the same as the solid lines in Figure 1c (4c).

Fig. 7.– PDF confidence contours (1, 2, and 3 σ) derived from the R98 SNe excluding the $z = 0.97$ one, for the time-independent Λ model. Panel $a)(b)$) ignores (accounts for) the H_0 and t_0 constraints (eqs. [3, 4]). The solid (dotted) lines use the non-informative $1/\Omega_0$ (flat) prior. The dotted lines in $a)(b)$) are the same as the dotted (solid) lines in Figure 5b. The dot-dashed lines are described in the caption of Figure 5. In the non-informative prior cases the likelihood function is computed down to $\Omega_0 = 0.01$.

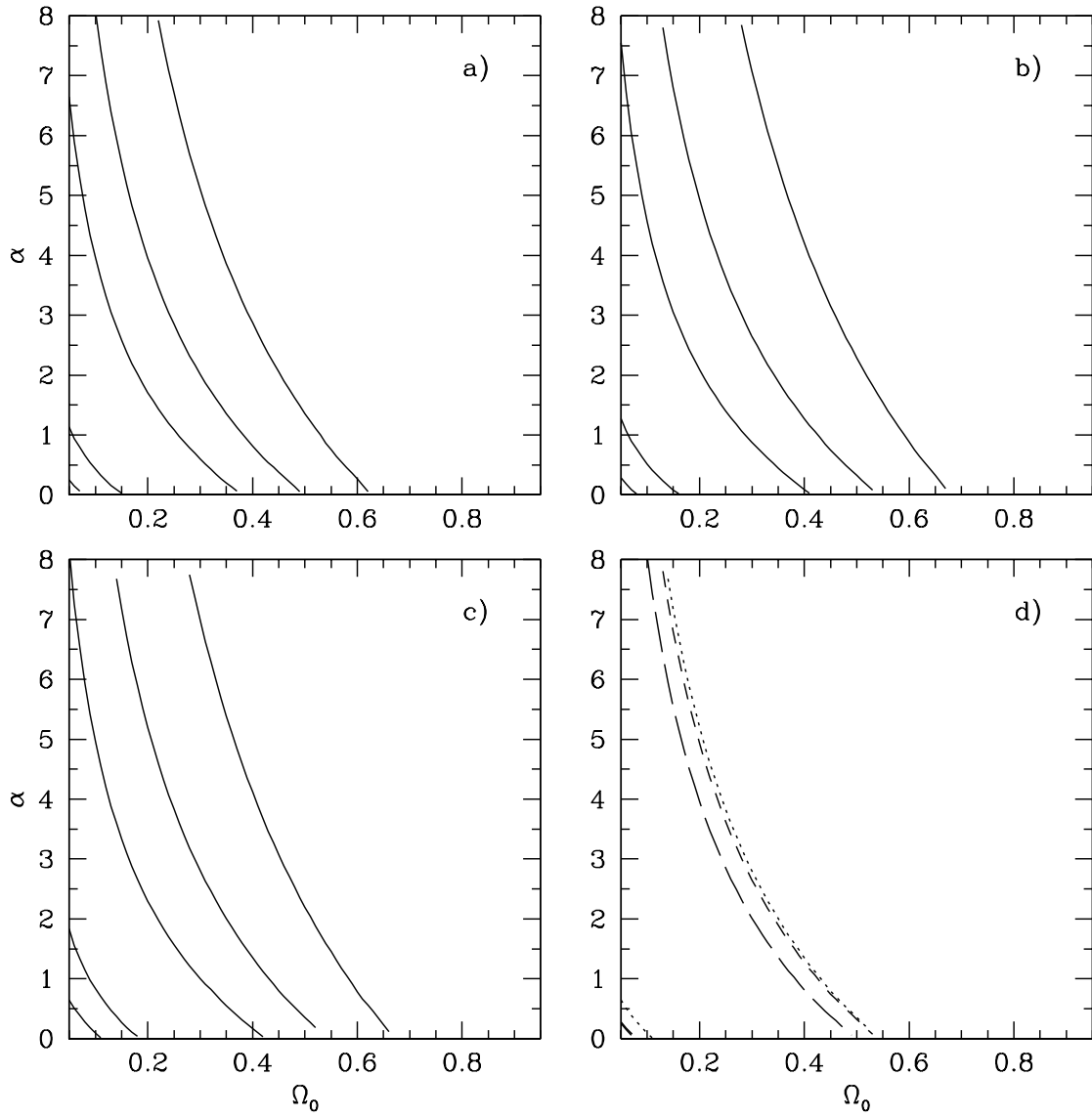


Figure 1

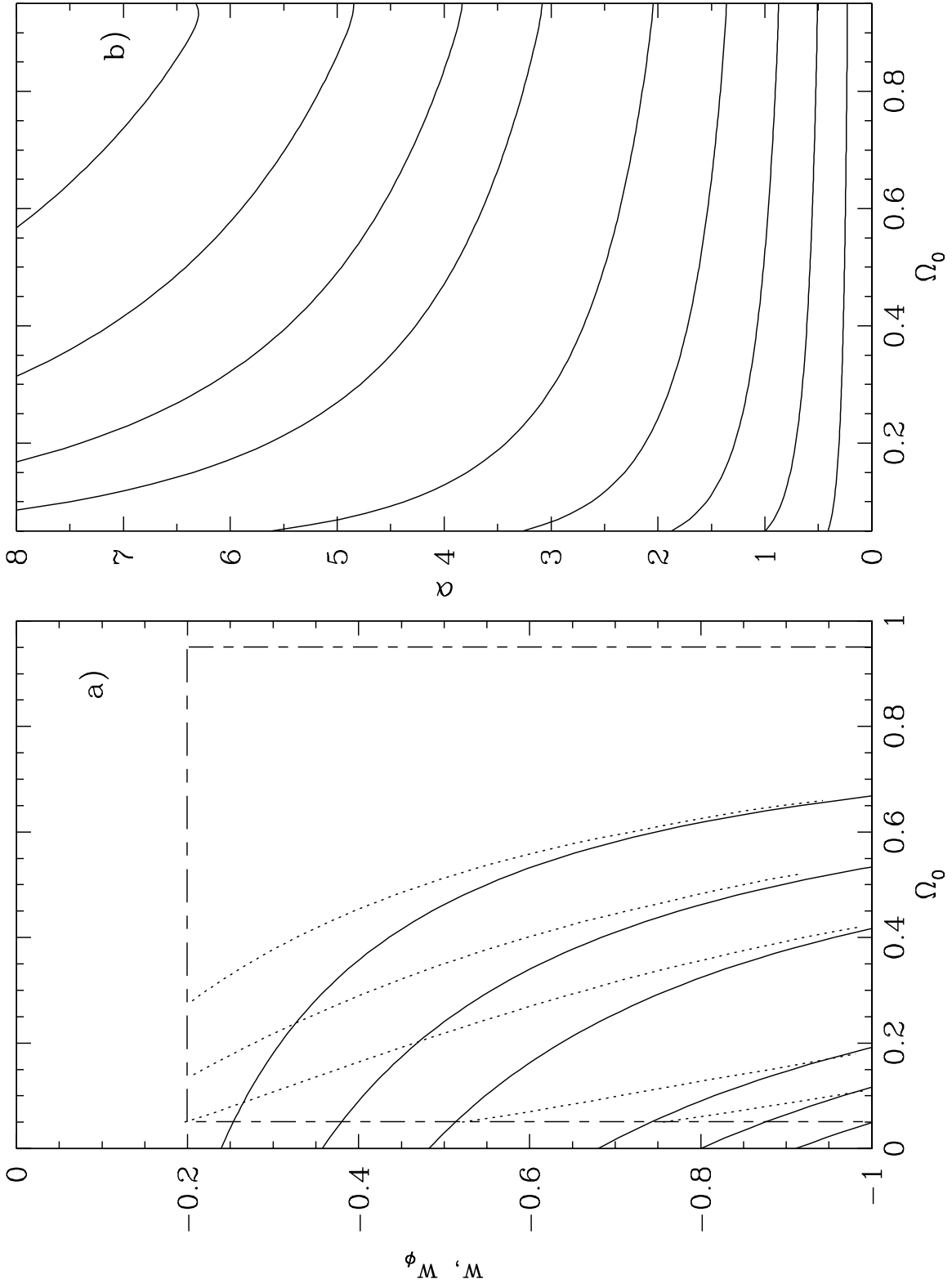


Figure 2

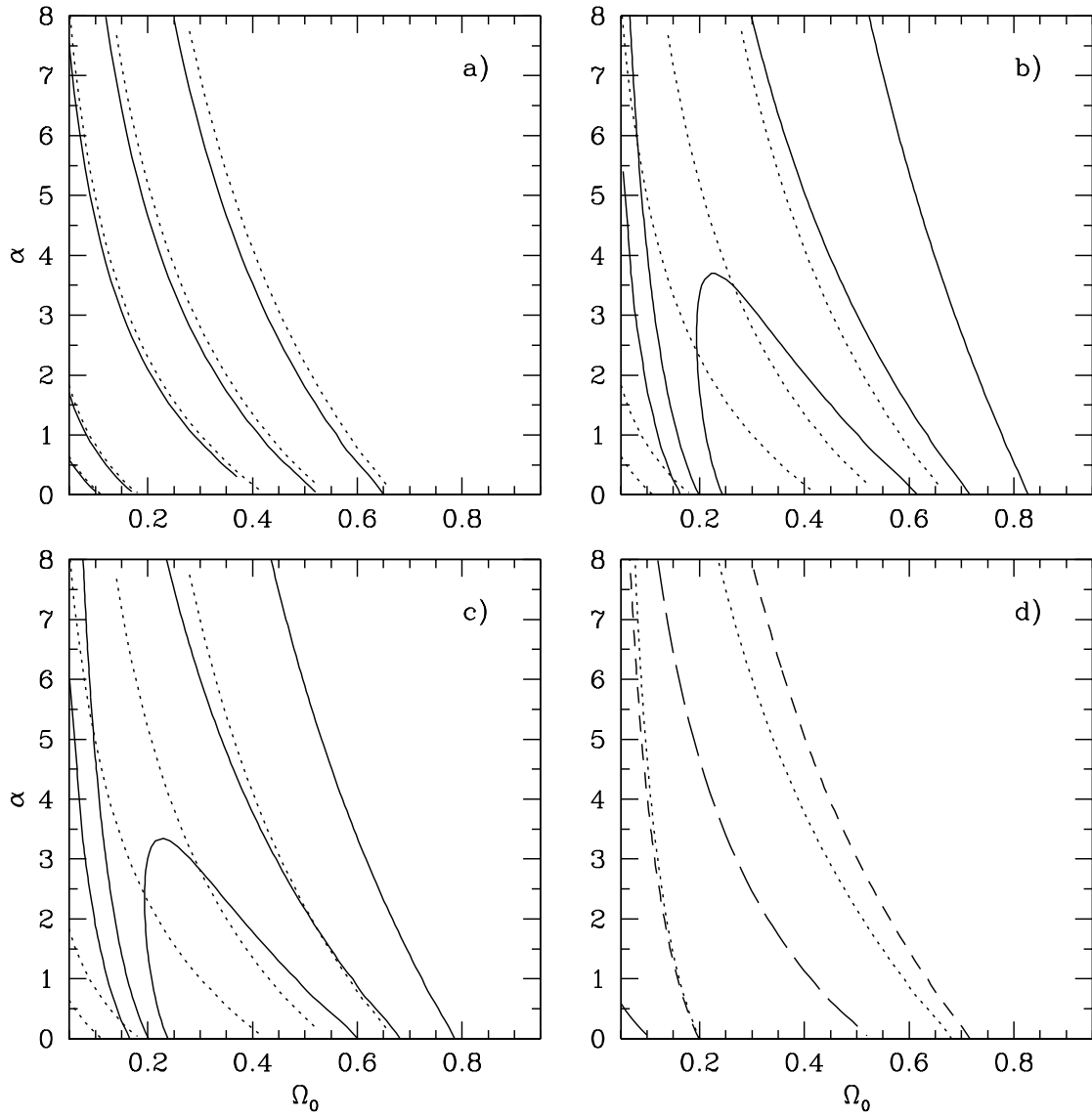


Figure 3

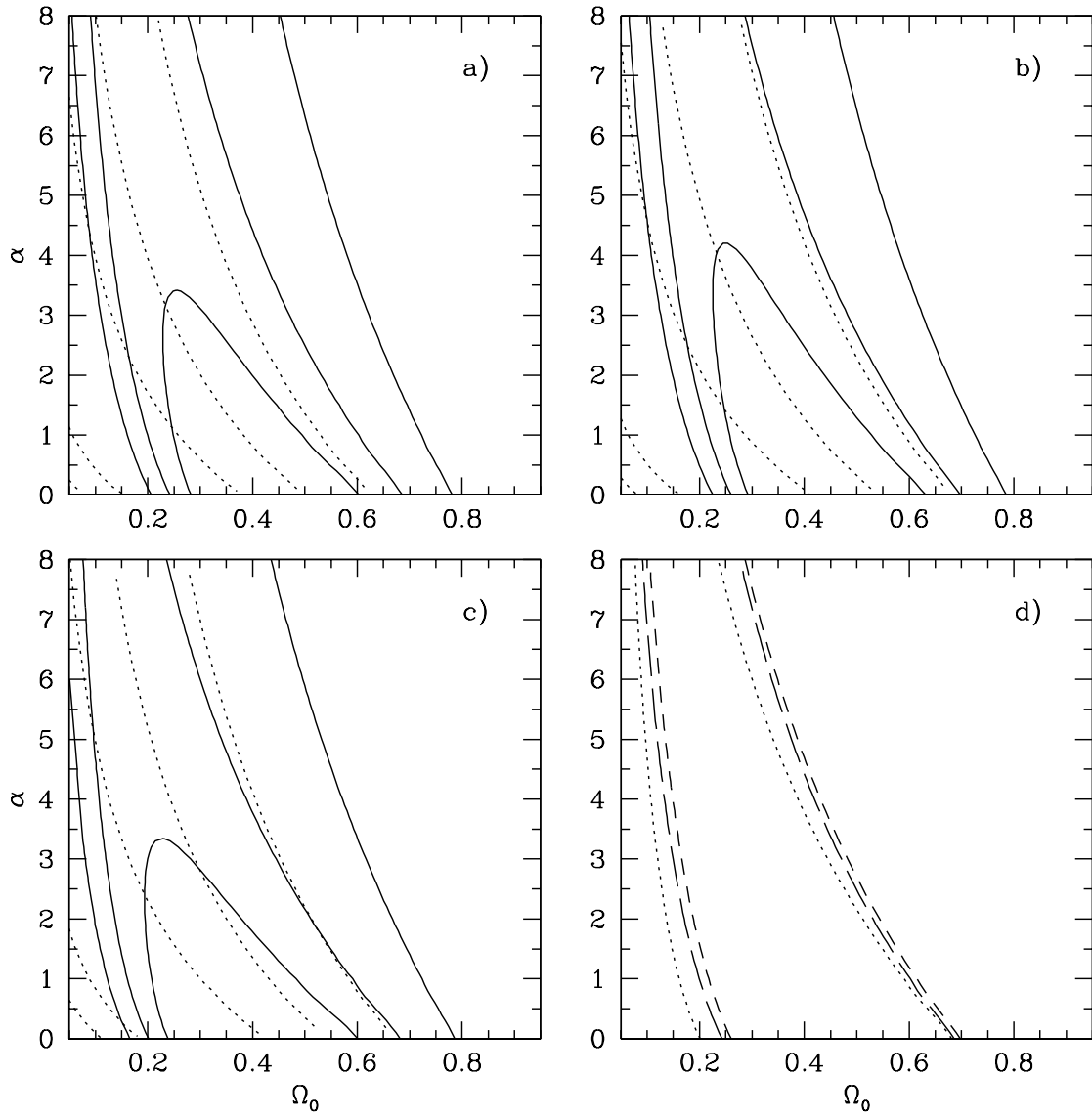


Figure 4

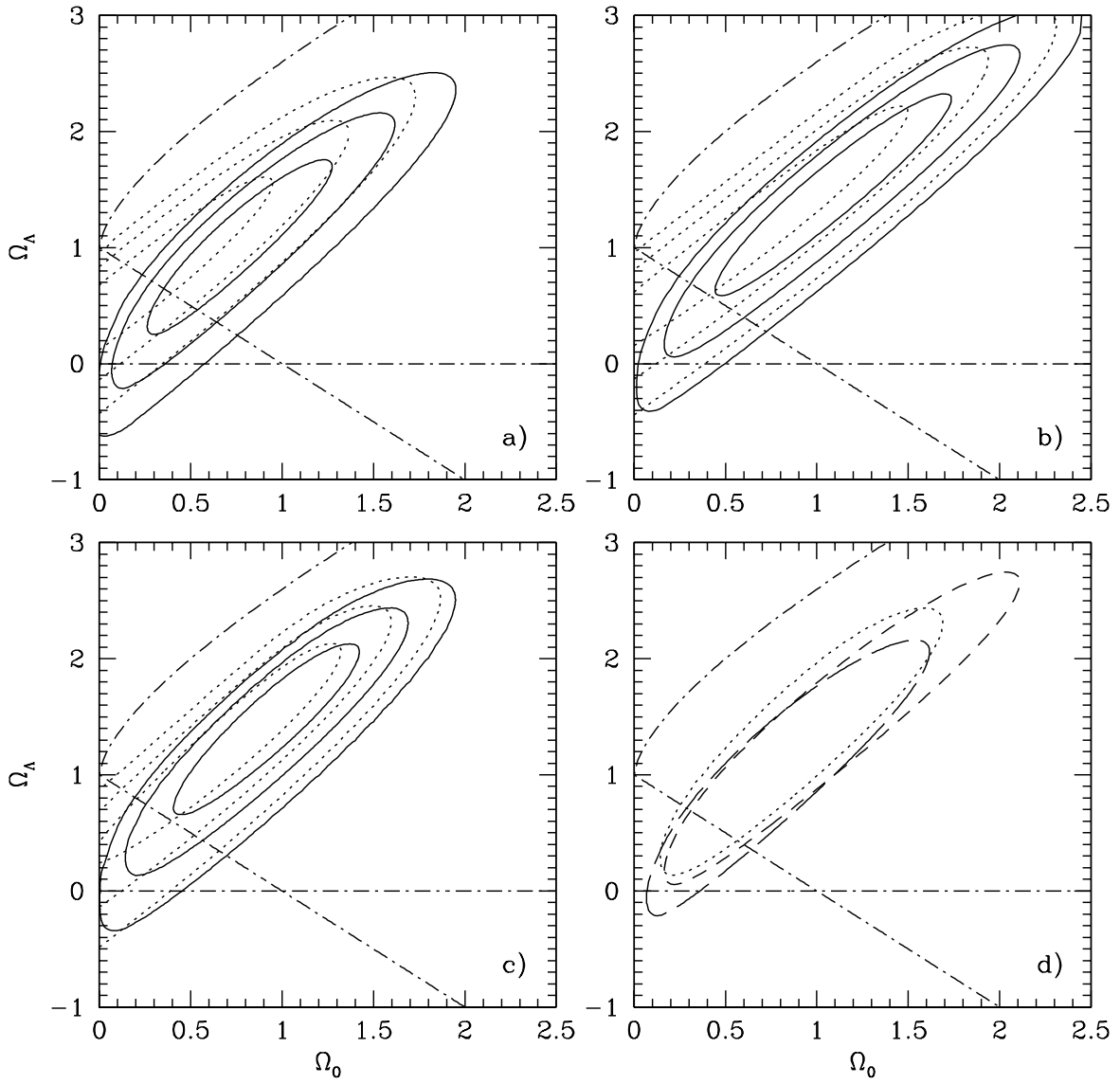


Figure 5

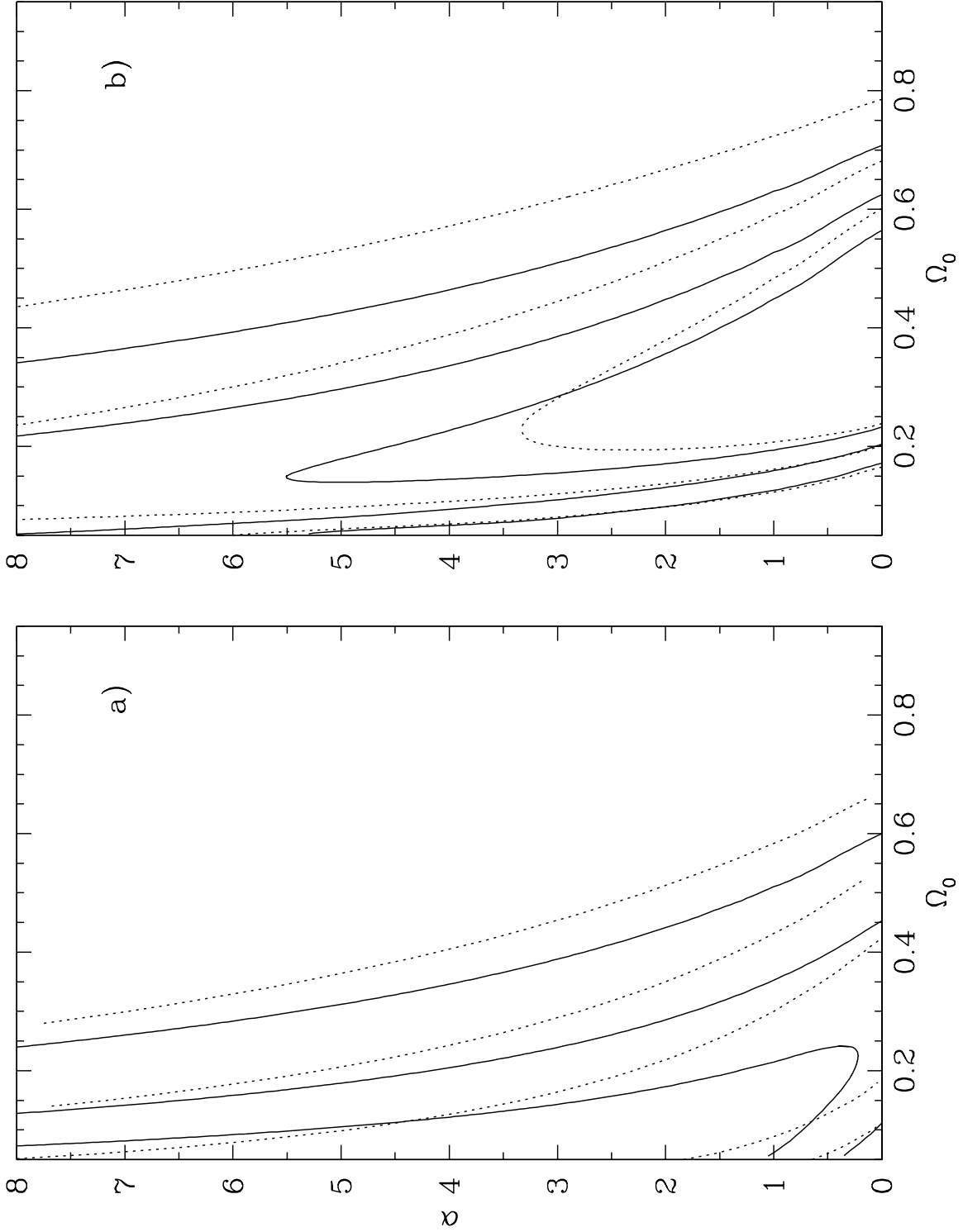


Figure 6

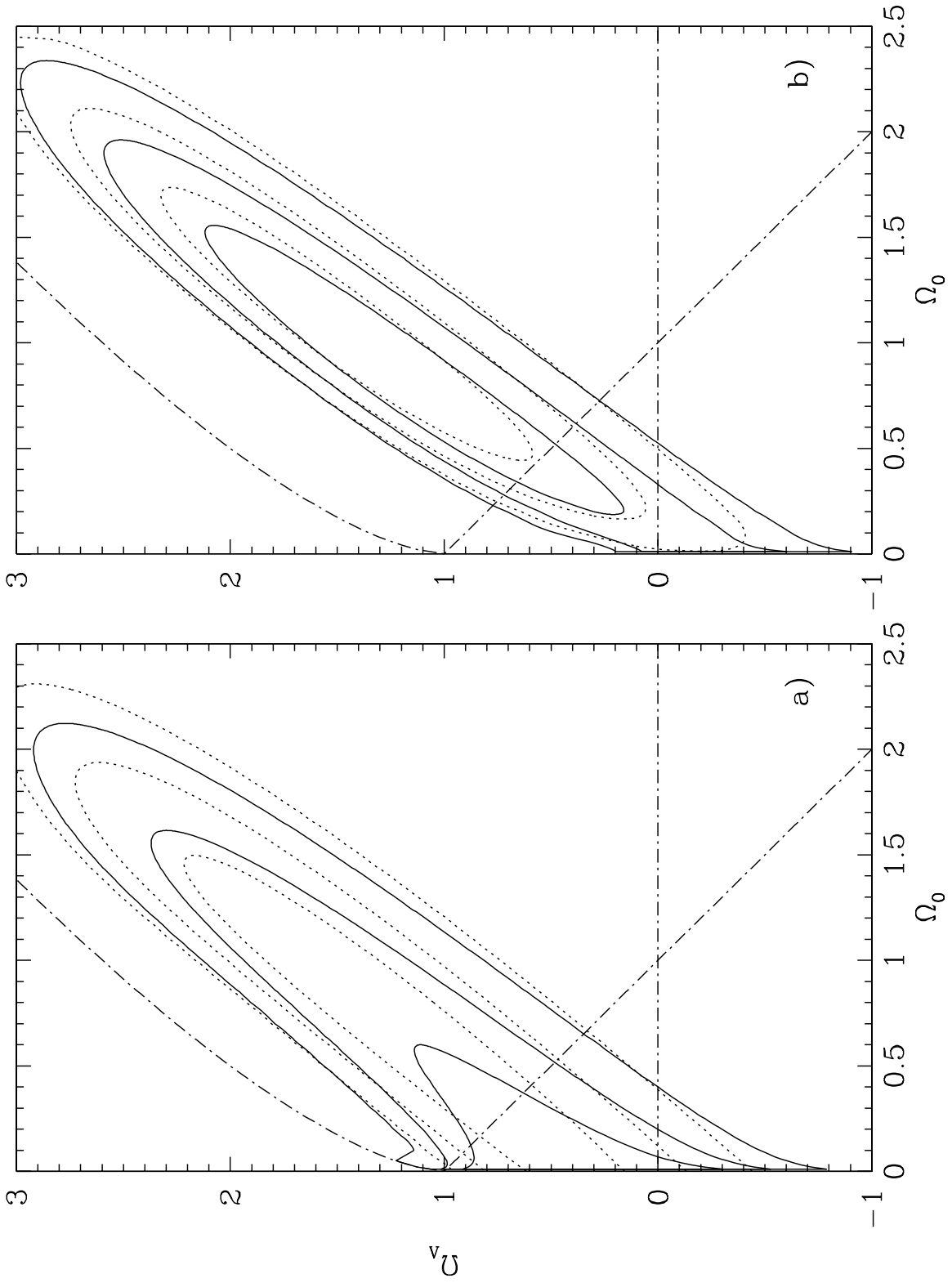


Figure 7